AGU PUBLICATIONS

JGR

Journal of Geophysical Research: Biogeosciences

RESEARCH ARTICLE
10.1002/2013JG002535

Special Section:
Experiment-Model Integration in Terrestrial Ecosystem Study: Current Practices and Future Challenges

Key Points:
- There is great uncertainty associated with carbon cycle simulations
- This uncertainty is reduced by calibrating models against globally observed data
- Parameter calibration reduces SOC loss under climate change

Supporting Information:
- Readme
- Figure S1
- Figure S2

Correspondence to:
O. Hararuk,
ohararuk@ou.edu

Citation:
Hararuk, O., J. Xia, and Y. Luo (2014), Evaluation and improvement of a global land model against soil carbon data using a Bayesian Markov chain Monte Carlo method, *J. Geophys. Res. Biogeosci.*, *119*, 403–417, doi:10.1002/2013JG002535.

Received 11 OCT 2013
Accepted 15 JAN 2014
Accepted article online 20 JAN 2014
Published online 28 MAR 2014

Evaluation and improvement of a global land model against soil carbon data using a Bayesian Markov chain Monte Carlo method

Oleksandra Hararuk[1], Jianyang Xia[1], and Yiqi Luo[1,2]

[1]Department of Microbiology and Plant Biology, University of Oklahoma, Norman, Oklahoma, USA, [2]Center for Earth System Science, Tsinghua University, Beijing, China

Abstract Long-term land carbon (C) cycle feedback to climate change is largely determined by dynamics of soil organic carbon (SOC). However, most evaluation studies conducted so far indicate that global land models predict SOC poorly. This study was conducted to evaluate predictions of SOC by the Community Land Model with Carnegie-Ames-Stanford Approach biogeochemistry submodel (CLM-CASA'), investigate underlying causes of mismatches between model predictions and observations, and calibrate model parameters to improve the prediction of SOC. We compared modeled SOC to the SOC pools from a globally gridded observation data product and found that CLM-CASA' on average underestimated SOC pools by 65% (r^2 = 0.28). We applied data assimilation to CLM-CASA' to estimate SOC residence times, C partitioning coefficients among the pools, and temperature sensitivity of C decomposition. The model with calibrated parameters explained 41% of the global variability in the observed SOC, which was substantial improvement from the initial 27%. The SOC and litter C feedback to changing climate differed between models with original and calibrated parameters: after 95 years of climate change (2006–2100), soils released 48 Pg C less in the calibrated than in the noncalibrated model and litter released 6.5 Pg C less in the calibrated than the noncalibrated model. Thus, assimilating estimated soil carbon data into the model improved model performance and reduced the amount of C released under changing climate. To further reduce the uncertainty in the soil carbon prediction, we need to explore alternative model structures, improve representation of ecosystems, and develop additional global datasets for constraining model parameters.

1. Introduction

Soils contain a large fraction of ecosystem carbon (C) [*House et al*., 2002], which can be affected by climate change [*Kirschbaum*, 1995]. Accurate prediction of soil organic C (SOC) content is important, as emission of CO_2 from soils greatly depends on the amount of carbon stored in it [*Luo and Zhou*, 2006]. Being a greenhouse gas, naturally and anthropogenically emitted CO_2 likely leads to climate warming [*Houghton et al*., 2001], which may further stimulate net release of soil carbon, forming a positive feedback loop between carbon cycle and climate warming [*Friedlingstein et al*., 2006; *Luo*, 2007; *Melillo et al*., 2002; *Oechel et al*., 2000; *Rustad et al*., 2001]. Analysis of the output generated by 11 Earth system models (ESMs) participating in the fifth Coupled Model Intercomparison Project (CMIP5) [*Taylor et al*., 2011] illustrates the uncertainty in the simulated SOC, which, despite the similarities in model structures, varies sixfold among the models with the estimates ranging from 510 to 3040 Pg C [*Todd-Brown et al*., 2013]. Only six out of 11 model estimates were within the range of the Harmonized World Soil Database (HWSD) estimate of 1260 Pg C (with a 95% confidence interval (CI) of 890–1660 Pg C), and none of the models' correlation coefficients for the grid-based comparisons between modeled and empirical SOC estimates exceeded 0.4 [*Todd-Brown et al*., 2013].

A few other studies that evaluated ESM's simulation of soil C stocks and dynamics indicated great differences between simulated and observed SOC stocks. *Kucharik et al*. [2000] evaluated the SOC stocks modeled by the Integrated Biosphere Simulator (IBIS) to be 1408 Pg C, which was lower than the estimate generated by International Geosphere-Biosphere Programme-Data and Information System (IGBP-DIS) (1567 Pg) [*Group*, 2000]. IBIS underpredicted soil C stocks by up to 8 kg C/m^2 in deserts, open shrublands, polar regions, and tropical forests and overpredicted soil C stocks by up to 11 kg C/m^2 in tundra regions. The second version of the IBIS model did not yield a better soil C fit [*Delire et al*., 2003]. *Thum et al*. [2011] evaluated

SOC in two global models: CBALANCE-JSBACH-ECHAM5-Model (Cba-JEM) [*Raddatz et al*., 2007; *Roeckner et al*., 2003] and Yasso07-JSBACH-ECHAM5-Model (Y07-JEM) [*Liski et al*., 2005; *Raddatz et al*., 2007; *Roeckner et al*., 2003]. The total global SOC simulated by Cba-JEM was 2853 Pg C and was higher than IGBP-DIS and HWSD estimates, whereas Y07-JEM simulated 1477 Pg C, which was lower than IGBP-DIS estimate, but within the range of the HWSD estimates [*Group*, 2000; *Todd-Brown et al*., 2013]. Both models overpredicted soil C in the northern conifer forests, tropical forests, grasslands, and savannas and underpredicted soil C in taiga regions. These differences in simulated SOC pools are likely propagated in the ESMs and cause substantial uncertainties in modeled carbon climate feedback [*Friedlingstein et al*., 2006].

ESM structures for simulating terrestrial carbon cycle are highly similar: they partition the photosynthetically fixed C among the live and dead carbon pools, from which C escapes via autotrophic or heterotrophic respiration [*Todd-Brown et al*., 2013; *Weng and Luo*, 2011]. *Todd-Brown et al*. [2013] showed that the differences in simulated SOC stocks among the models are mainly caused by their parameterizations. Parameter calibration is a commonly practiced procedure in model development, and parts of global land models have been calibrated with the site level data [*Kuppel et al*., 2012; *Wang et al*., 2007]. Calibration of land models against global data sets has not been widely implemented largely due to computational cost and methodological difficulty. For example, because of the lengthy spin-up, calibration of ESM parameters associated with soil carbon pools is computationally costly [*Rayner et al*., 2005]. Methodological difficulty arises from the fact that soil C content is a convoluted product of net primary productivity (NPP), C partitioning coefficient from plant litter to soil C pools, and SOC residence time [*Luo et al*., 2003; *Xia et al*., 2013; *Zhou and Luo*, 2008]. Even with the fixed NPP, same SOC content can be achieved by many combinations of C partitioning coefficients from plant litter to soil pools and SOC residence times (see Figure S1 in the supporting information). In a model with three soil C pools and nine other C pools (plant and litter) that contribute to the soil pools, it is difficult to identify the right set of parameters to adjust so as to make the simulated SOC stocks match closely to the observed ones.

Data assimilation techniques for parameter estimation have been successfully applied in the carbon cycle research at ecosystem, regional, and global scales. *Wu et al*. [2009] demonstrated significant improvement in modeled net ecosystem exchange (NEE) after applying conditional inversion method to the flux-based ecosystem model (FBEM) to integrate observed NEE data into FBEM at Harvard forest. At the same site, *Keenan et al*. [2012] assimilated 15 carbon pool and flux data sets into Forest Biomass, Assimilation, Allocation, and Respiration (FoBAAR) model to constrain 42 model parameters using adaptive multiple constraints Markov chain Monte Carlo optimization and were able to significantly reduce the forecast uncertainty of the C pool dynamics. *Xu et al*. [2006] used Bayesian Markov chain Monte Carlo technique to assimilate six carbon data sets from Duke Forest into the Terrestrial Ecosystem model to constrain C residence times and partitioning coefficients, producing good prediction of soil respiration, foliage biomass, and woody biomass.

On the regional scale, *Zhou and Luo* [2008] successfully constrained ecosystem residence times against regional data of biomass, net primary production (NPP), litter and soil C across the continental USA by using genetic algorithm to find the best parameters. *Zhou et al*. [2009] and *Ise and Moorcroft* [2006] presented global constrained SOC temperature sensitivities resulting from assimilating global soil C data [*Group*, 2000] into C cycle models. *Smith et al*. [2013] developed a fully data-informed C cycle model and generated C cycle projections with the parameter and structural uncertainties propagated in time.

Despite the obvious advantages to data assimilation for calibrating model parameters, not much research has been carried out with global land models due to their complexity. Meanwhile, the modeling community still focuses on including more processes into ESMs to represent the C cycle as realistically as possible [*Koven et al*., 2009, 2011; *Lawrence et al*., 2011; *Luo et al*., 2009; *Oleson et al*., 2008]. It is equally important to develop the capacity to calibrate models to improve their predictive ability. In this study we take advantage of Bayesian Markov chain Monte Carlo (MCMC) to (1) calibrate the C cycle component of CLM-CASA', (2) identify the regions with the highest uncertainty in SOC, (3) gain insight about the model structure through maximum likelihood parameter estimates and their correlations, (3) generate data-constrained estimates of C residence time, and (4) generate uncertainties of SOC change under climate change.

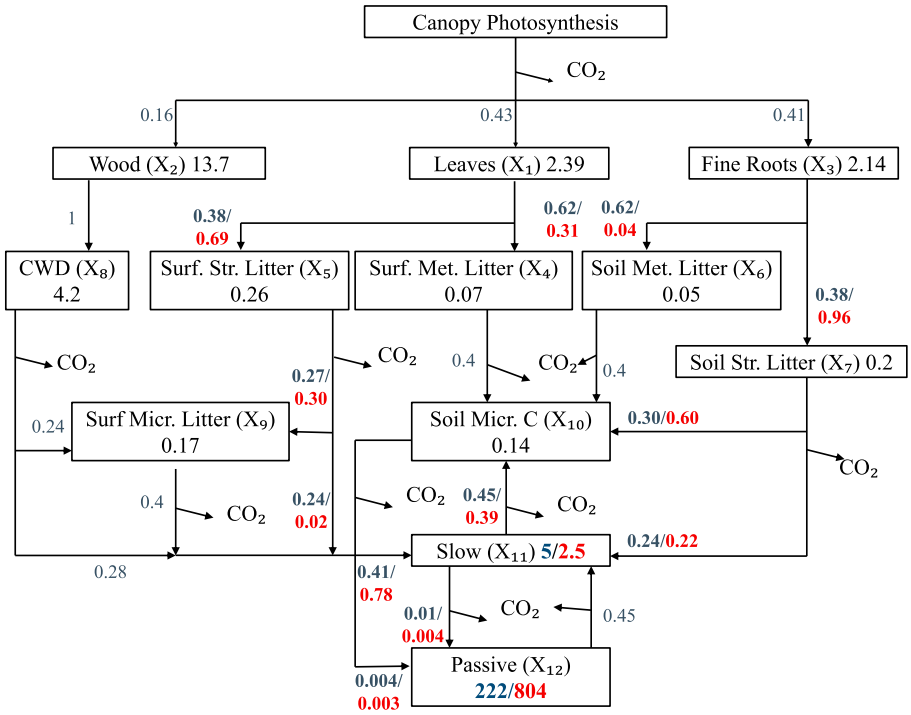

Figure 1. CLM-CASA' model structure and global parameter averages. Carbon enters the system through photosynthesis and is partitioned among three live pools. From the live pools carbon is transferred to the five litter pools, and from the litter pools it is transferred to the three soil pools. Values in the boxes are pool residence times; values outside the boxes are partitioning coefficients (values in blue are initial model values, values in red are results of parameter optimization). After data assimilation, soil passive C residence time increased by 36 years, whereas slow C residence time decreased by 2.1 years; compared to initial values, more C was transferred to soil C pools from soil litter and less C is transferred to soil C from surface litter.

2. Methods

2.1. CLM-CASA' and Its C-Only Version for Data Assimilation

In this study we calibrated Community Land Model coupled with Carnegie-Ames-Stanford Approach biogeochemistry submodel (CLM-CASA') [*Oleson et al.*, 2004, 2008; *Parton et al.*, 1993]. CLM-CASA' consists of biogeophysics and biogeochemistry submodels. Biogeophysics submodel simulates solar and longwave radiation dynamics in vegetation canopy and soil; momentum and turbulent fluxes from canopy and soil; heat transfer in soil and snow layers; hydrology of canopy, soil, and snow; stomatal physiology, and photosynthesis (more details can be found in [*Oleson et al.*, 2004, 2008]). Biogeochemistry submodel simulates carbon transfer among various plants, litter, and soil pools (Figure 1) [*Parton et al.*, 1993]. Change in carbon content in each pool is determined by a balance between influx into and efflux from the pool. Carbon influx into the ecosystem is defined by NPP, which is partitioned among three live biomass pools. Carbon efflux is heterotrophic respiration (autotrophic respiration in CLM-CASA' is assumed to be 50% of gross primary product) as determined by decomposition rate of organic C in each pool. Heterotrophic respiration is influenced by environmental conditions (specifically, temperature and soil moisture) as well as soil texture, tissue lignin, and tissue available nitrogen content.

Based on the theoretical analysis, carbon cycle components of any land models can be represented by a matrix equation (i.e., a set of carbon input-output equations) [*Luo and Weng*, 2011; *Luo et al.*, 2003; *Xia et al.*, 2013] as

$$\frac{d\boldsymbol{X}(t)}{dt} = \mathbf{A}\xi(t)\mathbf{C}\boldsymbol{X}(t) + \boldsymbol{B}U(t) \quad (1)$$

where $\frac{d\boldsymbol{X}(t)}{dt}$ is the change in C pools at each time step; $\xi(t)$ is the diagonal matrix of environmental scalars, which represents the influence of climate on mortality or decomposition rate of organic C in each pool in a grid cell (the elements of $\xi(t)$ for all nonlive pools are the same); **A** is a matrix of partitioning coefficients among C pools, which is influenced by soil texture, lignin, and tissue lignin to nitrogen ratio; **C** is the diagonal

matrix of baseline C exit rates at a given temperature (25°C in CLM-CASA'); $\boldsymbol{X}(t)$ is a vector of C pools; $\boldsymbol{B}$ is the vector of partitioning coefficients of NPP to the three live biomass pools; and $U(t)$ is NPP.

Based on equation (1), we extracted the carbon cycle component of CLM-CASA' into a set of equations that described carbon transfer among pools, solved the steady state solution for the set of equations, and encoded them into MATLAB to perform data assimilation. Steady state solution for each grid cell was calculated as proposed by *Xia et al*. [2012]:

$$X_{ss} = -\left(\mathbf{A}\,\overline{\xi}\,\mathbf{C}\right)^{-1}\overline{\boldsymbol{B}}\,\overline{U} \tag{2}$$

where $\overline{\xi}$, $\overline{\boldsymbol{B}}$, and $\overline{U}$ were long-term averages of the environmental scalars, C partitioning among the three live pools, and NPP correspondingly. Before proceeding to data assimilation we verified the MATLAB version of CLM-CASA' by comparing its simulated soil C content with that of the original model. As illustrated in Figure S2, steady state soil C simulated by the original CLM-CASA' model matched closely to that produced by the MATLAB version despite that the latter used the semianalytic spin-up approach [*Xia et al*., 2012]. Extracting the carbon component from the original model for data assimilation saved computational time and made it easier to fit our data assimilation workflow.

2.2. Data Assimilation for Parameter Estimation

To calibrate parameters associated with soil C we used Bayesian probabilistic inversion, which states that posterior probability density functions of parameters can be obtained from prior knowledge about the parameters and the error between model and observations. According to *Mosegaard and Sambridge* [2002], Bayesian inversion can be summarized by the following equation:

$$p(c|Z) = v_c \times p(Z|c) \times p(c) \tag{3}$$

where $p(c|Z)$ is posterior probability density function of model parameters c; $p(Z|c)$ is a likelihood function of parameters c; $p(c)$ is prior probability density function of parameters c; v_c is a normalization constant. We assumed that the prediction errors were normally distributed and uncorrelated, hence, the likelihood function, $p(Z|c)$, was calculated as follows:

$$p(Z|c) = v_L \times \exp\left\{-\sum_{i=1}^{k}\frac{(Z_i - X_i)^2}{2\sigma_i^2}\right\} \tag{4}$$

where Z_i is soil C reported by IGBP-DIS at ith grid cell, X_i is soil C simulated by CLM-CASA' at a corresponding grid cell; σ_i^2 is the variance of a measurement at a grid cell; k is the total number of grid cells; and v_L is a constant. The issue of uncertainty in the global-gridded data products is much understudied, and IGBP-DIS database, like many other global-gridded data products, does not include the uncertainty estimates. In light of the absent uncertainties we employed a concept used in *Harmon and Challenor* [1997] and assumed a standard deviation of 30% of a reported value at each grid cell, which we then used to calculate the variance.

To generate the posterior distributions we first specified the priors of the parameters to be uniformly distributed over the intervals specified in Table 1. We put constraints on parameters based on the literature, educated guess, and hypothesis testing. For instance, temperature sensitivity was varied between 1, assuming that respiration was insensitive to temperature, and 3 (average temperature sensitivity calculated from the global soil respiration database) [*Bond-Lamberty and Thomson*, 2012]. The minima for maximum turnover rates in slow and passive pools were within the reported range [*Parton et al*., 1993, 2010]; however, because the maximum turnover rates for slow SOC pool in CLM-CASA' was the highest reported, we made upper limits in this study 2.5 times the original value to test whether the maximum turnover rate could be higher on the global level than those reported to date. The upper limit for the passive SOC turnover rate was set at 0.005 years^{-1}, which was higher than the rate used in *Parton et al*. [1993] by 0.0005 years^{-1}. Literature search yielded no information about the range for the other 17 parameters from Table 1, therefore, we assigned the limits to the parameters so that they would preserve the original relationship with the dependent variables (e.g., soluble fraction, structural lignin, clay, and sand), but adjust the degree of influence of the dependent variables on a C partitioning coefficient. As an additional constraint, C partitioning coefficients had to be a value between 0 and 1, and the sum of partitioning coefficients for C efflux from the same pool could not be larger than 1.

Once we specified parameter ranges, we used adaptive Metropolis (AM) algorithm [*Haario et al*., 2001], a Markov chain Monte Carlo method, to sample from the posterior parameter distribution. To generate a parameter chain,

Table 1. CLM-CASA' Parameter Characteristics[a]

Parameter Description	Symbol	Prior			MLE	G-R	Lower 95%	Upper 95%
		Minimum $\times 10^{-3}$	Maximum $\times 10^{-3}$	Value $\times 10^{-3}$	$\times 10^{-3}$		Bounds $\times 10^{-3}$	Bounds $\times 10^{-3}$
Exit rate from slow pool, (years^{-1})	c(11,11)	100	500	200	400	1.00	287	488
Exit rate from passive pool, (years^{-1})	c(12,12)	1	5	4.5	1	1.00	1.04	2
Temperature sensitivity of C decomposition	Q_{10}	1000	3000	2000	1837	1.00	1751	1989
Labile C fraction effect on C partitioning from leaves to surface metabolic litter	w_1	0	1000.1	1000	503	1.00	120	920
Labile C fraction effect on C partitioning from roots to soil metabolic litter	w_2	0	1000.1	200	75	1.00	13	366
Partitioning from surface structural to surface microbial pool if no lignin in surface structural litter	l_1	350	2300	400	461	1.00	369	811
Lignin effect on partitioning from surface structural litter to surface microbial litter	l_2	0	700	400	462	1.00	166	674
Lignin effect on partitioning from surface structural litter to soil slow pool	l_3	0	800	700	59	1.00	11	302
Partitioning from soil structural to soil microbial pool if no lignin in soil structural litter	l_4	400	700	450	648	1.00	573	695
Lignin effect on partitioning from soil structural litter to soil microbial pool	l_5	0	900	450	135	1.00	23	557
Lignin effect on partitioning from soil structural litter to soil slow pool	l_6	0	900	700	654	1.00	334	875
C partitioning from soil microbial pool to slow pool if no sand or clay	t_1	19	750	169	655	1.00	527	741
Clay effect on C partitioning from soil microbial pool	t_2	0	30	5.44	25	1.00	17	30
Sand effect on C partitioning from soil microbial to slow pool	t_3	0	1000	678	343	1.00	57	844
Combined effect of sand and clay on C partitioning from soil microbial pool	t_4	0	100	22	67	1.00	34	96
C partitioning from soil microbial to passive pool if no sand or clay	t_5	0.1	0.8	0.51	0.39	1.00	0.14	0.73
Sand effect on C partitioning from soil microbial to passive pool	t_6	0	30	2.04	9	1.00	3.26	21
Clay effect on C partitioning from slow pool to passive pool	t_7	0	700	4.05	22	1.00	11	52
C partitioning from slow to passive pool if no clay	t_8	0	20	14	1	1.01	0.11	3
C partitioning from slow to soil microbial pool if no clay	t_9	300	700	449	384	1.00	314	599

[a]MLE is maximum likelihood estimate, and G-R is the result of Gelman-Rubin chain convergence diagnostics.

we ran AM algorithm in two steps: proposing step and a moving step. In the proposing step, a new parameter set c^{new} was generated from a previously accepted parameter set c^{k-1} through a proposal distribution ($c^{new}|c^{k-1}$). In the moving step, a probability of acceptance $P(c^{k-1}|c^{new})$ was calculated as in the following [*Marshall et al*., 2004]:

$$P\left(c^{k-1}\middle|c^{new}\right) = \min\left\{1, \frac{p(Z|c^{new})p(c^{new})}{p(Z|c^{k-1})p(c^{k-1})}\right\} \tag{5}$$

The value of $P(c^{k-1}|c^{new})$ was then compared with a random number U from 0 to 1. Parameter set c^{new} was accepted if $P(c^{k-1}|c^{new}) \geq U$, otherwise c^k was set to c^{k-1}.

The AM algorithm requires an initial parameter covariance matrix, which we generated from a test run of 50,000 simulations using a uniform proposal distribution following the example in *Xu et al*. [2006]:

$$c^{new} = c^{k-1} + r \times \frac{c^{max} - c^{min}}{D} \tag{6}$$

where c^{max} and c^{min} are upper and lower parameter limits, r is a random number between -0.5 and 0.5, and $D = 5$. Out of 50,000 simulations, the test run accepted about 2500 updated samples. We constructed a covariance matrix C_0 on the basis of the test run and modified the proposal step to be

$$c^{new} = N\left(c^{k-1}, C_k\right) \tag{7}$$

$$C_k = \begin{cases} C_0 & k \leq k_0 \\ s_d \mathrm{Cov}(c_0, \ldots, c_{k-1}) & k > k_0 \end{cases} \tag{8}$$

where $k_0 = 2000$ and $s_d = 2.38/\sqrt{20}$ [*Gelman et al*., 1996].

We made five parallel runs starting at dispersed initial points in the parameter space, each run contained 1,000,000 simulations. During each simulation we solved equation (2) with newly proposed parameters and proceeded to the moving step. We discarded the first half of the simulations (as burn-in phase) and tested the second half for convergence to stationary distributions with Gelman-Rubin diagnostics [*Gelman and Rubin*, 1992].

2.3. Parameters to be Estimated

Soil C content is determined by soil C influx (proportional to NPP) and its residence time, or the inverse of the turnover rate [*Luo et al*., 2003]. The point-by-point comparisons of the NPP produced by CLM-CASA' and the observed NPP from Ecosystem Model Data Intercomparison Initiative data set [*Olson et al*., 2001] showed good agreement between modeled and observed NPP [*Randerson et al*., 2009]. Due to this good agreement we used modeled NPP to drive the CASA' biogeochemistry submodel and focused on improving the SOC through calibrating the parameters associated with turnover rates of carbon pools and C partitioning coefficients among pools as influenced by climate, tissue lignin, available nitrogen, and soil texture. Specifically, we calibrated the baseline C exit rates from slow and passive C pools (these two parameters strongly regulated SOC pool size due to their long residence times), temperature sensitivity of heterotrophic respiration (Q_{10}), and the parameters in (i.e., elements of) matrix **A**, which we described in the following equations:

$$a(4,1) = w_1 * \mathrm{lf} \tag{9}$$

$$a(5,1) = 1 - a(6,3) \tag{10}$$

$$a(6,3) = w_2 * \mathrm{lf} \tag{11}$$

$$a(7,3) = 1 - a(6,3) \tag{12}$$

where $a(4,1)$ is the partitioning coefficient from leaves to surface metabolic litter; $a(5,1)$ is the partitioning coefficient from leaves to surface structural litter; $a(6,3)$ is the partitioning coefficient from roots to soil metabolic litter; $a(7,3)$ is the partitioning coefficient from roots to soil structural litter; lf is the labile C fraction in leaves and roots at a given grid cell; and w_1 and w_2 are empirical coefficients.

$$a(9,5) = l_1 - l_2 * \mathrm{sl} \tag{13}$$

$$a(11,5) = l_3 * \mathrm{sl} \tag{14}$$

$$a(10,7) = l_4 - l_5 * \mathrm{sl} \tag{15}$$

$$a(11,7) = l_6 * \mathrm{sl} \tag{16}$$

where $a(9,5)$ is C partitioning coefficient from surface structural litter to surface microbial pool; $a(11,5)$ is C partitioning coefficient from surface structural litter to soil slow pool; $a(10,7)$ is C partitioning coefficient from soil structural litter to soil microbial pool; $a(11,7)$ is C partitioning coefficient from soil structural litter to soil slow pool; sl is structural lignin content in the structural litter pools in a given grid cell expressed as a fraction of 1; and l_1 through l_6 are empirical parameters.

$$a(11,10) = t_1 - t_2 * \mathrm{clay} + t_3 * \mathrm{sand} - t_4 * \mathrm{clay} * \mathrm{sand} \tag{17}$$

$$a(12,10) = t_5 + t_2 * \mathrm{clay} + t_6 * \mathrm{sand} - t_4 * \mathrm{clay} * \mathrm{sand} \tag{18}$$

$$a(12,11) = t_8 + t_7 * \mathrm{clay} \tag{19}$$

$$a(10,11) = t_9 - t_7 * \mathrm{clay} \tag{20}$$

where $a(11,10)$ is C partitioning coefficient from soil microbial to soil slow pool; $a(12,10)$ is C partitioning coefficient from soil microbial to soil passive pool; $a(12,11)$ is C partitioning coefficient from soil slow to soil passive pool; $a(10,11)$ is C partitioning coefficient from soil slow to soil microbial pool; clay and sand are the soil clay and sand fractions in a given grid cell; and t_1 through t_9 are empirical parameters. Those parameters together with their prior values are listed in Table 1.

2.4. Database

IGBP-DIS database provides a high-resolution (5 × 5 arc min) global map of soil C for the top 1 m of soil. The map is the result of linking the pedon records from the extensive Global Pedon Database [*Batjes*, 1995], which contains soil texture classes, terrain slopes, and 106 soil units, and FAO/UNESCO Digital Soil Map of the world (containing the above mentioned data in addition to pH, organic C and nitrogen, bulk density, cation exchange capacity, etc. [*FAO*, 1995]) by statistical bootstrapping. The database features data on soil bulk density, field capacity, thermal capacity, soil carbon, and nitrogen density. Many studies used the soil carbon data from this data set to produce new data sets [*House et al*., 2002], as an assessment of terrestrial C uptake [*Freibauer et al*., 2004], to evaluate models [*Delire et al*., 2003; *Kucharik et al*., 2000], and to improve models [*Ise and Moorcroft*, 2006; *Smith et al*., 2013; *Zhou et al*., 2009]. Prior to using the data set in the data assimilation routine, we randomly separated all the grid cells into halves similar to *Smith et al*. [2013]. One half of grid cells

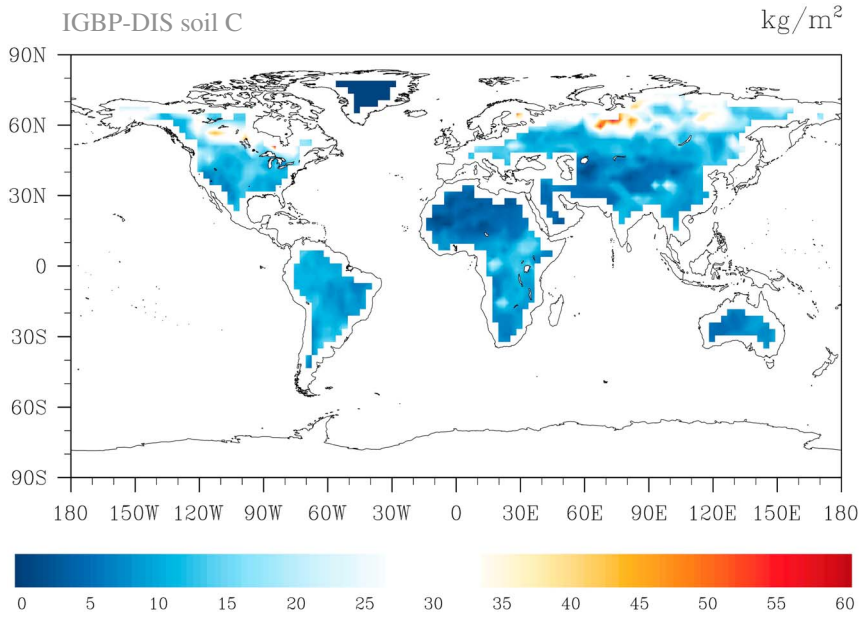

Figure 2. IGBP-DIS soil carbon distribution. Soil carbon varies from 0 kg/m^2 in deserts to 60 kg/m^2 in the northern regions.

was used for model calibration and the second group—for validation to avoid overfitting. All further discussion about the fit of modeled data to observed data will refer to the validation subsample of the data.

In this study, for the purpose of estimation of the parameters related to carbon processes, soil C in the IGBP-DIS database was assumed to be in a steady state. This assumption could not be verified at present because of the lack of time series data over the globe. However, *Zhou and Luo* [2008] researched parameter uncertainty resulting from the steady state assumption by calibrating parameters two times: with equilibrium SOC values and with SOC reduced 40% from the equilibrium values. Their finding was that the parameters obtained with the equilibrium assumption were within the margin of error of the parameters obtained after 40% reduction in soil C (except for the C partitioning coefficients from the soil pools), therefore, even with equilibrium assumption we were likely to constrain the parameters at their true values. Moreover, 40% from the steady state soil C content represents extreme cases as most of the disturbances do not cause such big changes in soil C. The steady state assumption made our MATLAB model version particularly effective for data assimilation as it used averaged values of environmental responses (scalars) to repeated environmental forcing [*Xia et al.*, 2012].

The litter lignin content was in CLM-CASA' by default: the plant-functional-type-level estimates of lignin were applied to Moderate Resolution Imaging Spectroradiometer-derived distribution of plant-functional types used in CLM [*Lawrence and Chase*, 2007; *Oleson et al.*, 2007]. Labile C pool fraction in roots was estimated by the CLM-CASA' model from the lignin to nitrogen ratio, and the latter, similar to litter lignin content, was by default assigned to each plant-functional type in CLM-CASA'. The maps of soil sand and clay content were originally developed by the International Geosphere-Biosphere Programme [*Group*, 2000] and were provided as a part of CLM-CASA' package.

2.5. Forward Analysis of Carbon Dynamics With Original and Optimized Parameters

After parameter calibration we ran forward simulations with the original and calibrated parameters and examined the change in ecosystems' responses to increasing temperature and atmospheric CO_2 concentrations. We used the Community Earth System Model (CESM) output for the Representative Concentration Pathway 8.5 (RCP8.5) experiment (specifically, temperature and live pool sizes) to drive the litter and soil C pools in CLM-CASA' with original and calibrated parameters. The CESM model output was provided as a part of Coupled Model Intercomparison Project Phase 5 (CMIP5) and could be accessed at (http://pcmdi9.llnl.gov). Over 95 years, CESM simulated a 3.5 K increase in mean global temperature and atmospheric CO_2 increase to 1150 ppm by the year 2100 [*Keppel-Aleks et al.*, 2013]. We ran the CASA' model forward in time starting from the year 2006 to 2100, using the average live pools, their residence times, and temperatures for the years 2006–2010 to generate initial litter and soil C pools using the semianalytical spin-up [*Xia et al.*, 2012].

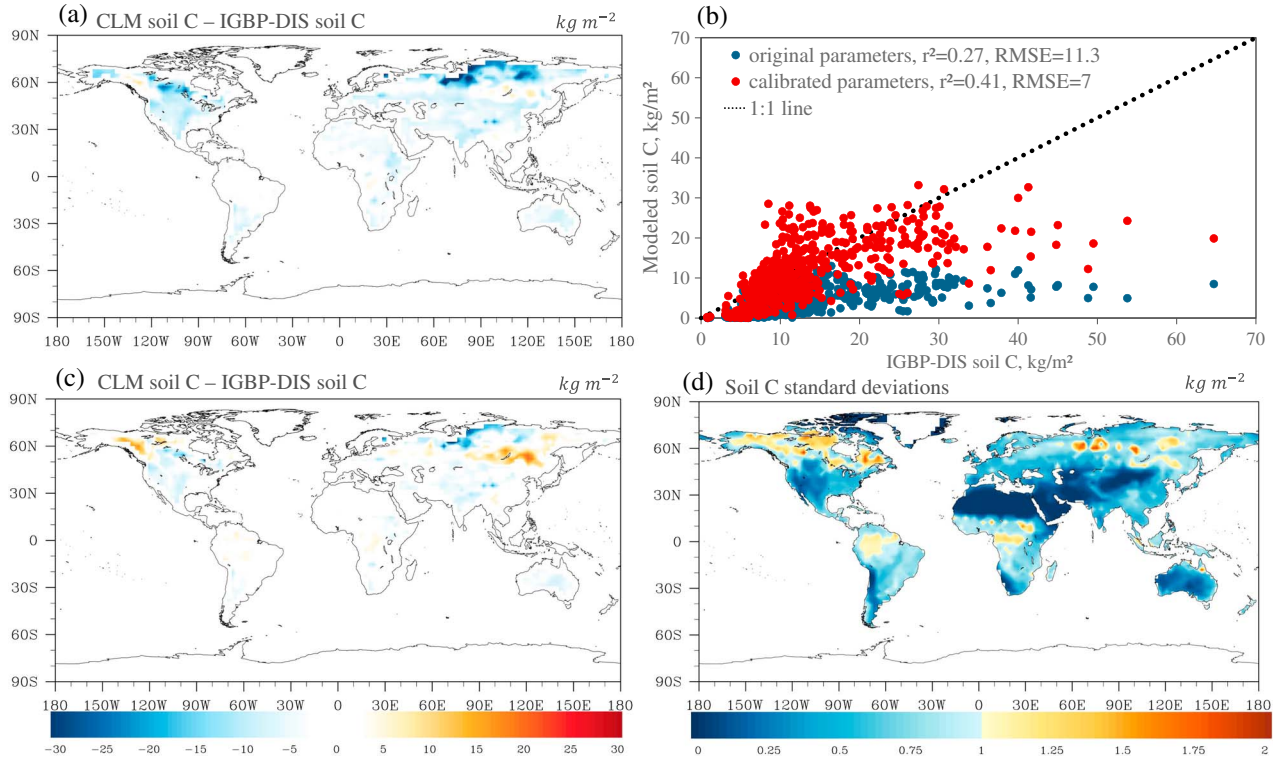

Figure 3. Spatial correspondence of CLM-CASA' produced SOC to the IGBP-DIS reported SOC (a, b) before and (b, c) after data assimilation, and (d) standard deviations in the modeled soil C after data assimilation. The points in Figure 3b represent the grid cell values. Model with default parameters explained 27% of variation in the observed soil C, whereas model with calibrated parameters explained 41% of variability in the observed soil C. The regions with highest uncertainty were located in the northern latitudes and in the tropics.

3. Results

3.1. Evaluation and Improvements of Modeled SOC

We estimated SOC pool sizes at steady states (equation (2)), which we then compared to observed SOC pools provided by IGBP-DIS global-gridded product (Figure 2b) [*Group*, 2000]. CLM-CASA' explained 27% of spatial variability in the observed data (Figures 3a and 3b). The model on average underestimated soil C pools by 8.8 kg/m^2 with the largest deviations in the northern regions, where soil C was underestimated by more than 30 kg/m^2 (Figure 3a). The root-mean-square error (RMSE) of CLM-CASA' was 11.34 kg/m^2.

3.2. Constrained Parameters Related to Soil Carbon Dynamics

All estimated parameters converged to stationary distributions as indicated by the Gelman-Rubin diagnostics [*Gelman and Rubin*, 1992] (Table 1). Assimilation of SOC data set into CLM-CASA' model resulted in tight constraints on temperature sensitivity of heterotrophic respiration (Q_{10}) and clay effect on C partitioning from slow to passive pool (t_7) (Figure 4). Sharp posterior distributions indicated that model predictions were highly sensitive to changes in those parameters, which agreed with the findings of *Post et al.* [2008]. Sand effect on C partitioning from soil microbial to passive pool (t_6) was also constrained within the prior values, however, its distribution was not as sharp as distributions of Q_{10} and t_7. Many posterior parameters were skewed against their assigned maximum or minimum values. This was especially the case for baseline passive C exit rate, which was skewed against its minimum value, suggesting that residence time of passive SOC under optimum environmental conditions was larger than 1000 years. *Parton et al.* [2010] assigned passive pool residence times up to 5000 years in DayCent model (a model with similar carbon submodel to CLM-CASA'). However, in the same study, they presented the improved model version, ForCent, which had the highest value of 1000 years, hence we did not increase the maximum boundary for baseline passive pool's residence time above 1000 years.

Many parameters associated with soluble fraction, structural lignin, and soil texture effects on C partitioning coefficients were skewed against their boundaries. For instance, posterior distribution of t_8, was skewed against its minimum (Figure 4), indicating increased effect of clay on C partitioning from slow to passive pool

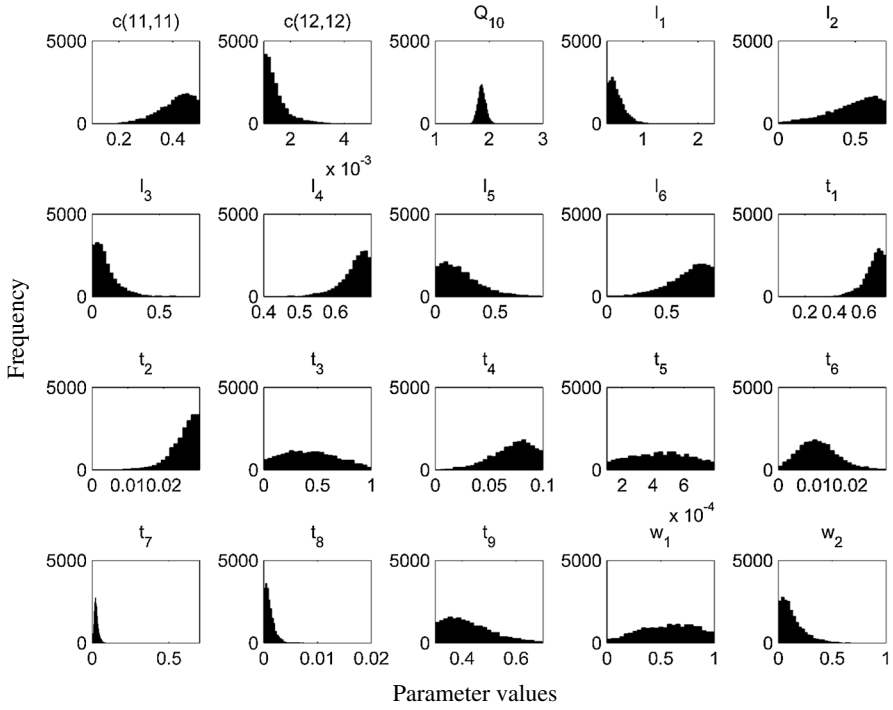

Figure 4. Frequency distributions of 20 calibrated parameters. The most constrained parameters were temperature sensitivity of heterotrophic respiration ($\mathbf{Q_{10}}$), clay effect on C partitioning from slow to passive pools ($\boldsymbol{t_7}$), and sand effect on C partitioning from soil microbial to passive pool.

as lower fraction would be transferred to passive pool in soils with low clay content (equation (20)). Skews of t_1 and t_2 against their maxima indicated that more C was transferred from fast to slow pool under low clay and sand content, and clay effect on C transfer from fast to slow and passive pools was larger than modeled originally (equations (17) and (18)). Skew of l_3 against its minimum indicated either no relationship between structural lignin and C partitioning between surface structural and slow pools, or very low C transfer between these pools (equation (14)). Similarly, calibration revealed the absence of relationship between labile C fraction and C transfer from roots to soil litter pools as indicated by the skew in w_2, however, it could also mean that under the given model formulation, all C from roots had to go to soil structural litter to reproduce spatial patterns of SOC. Some of the parameter skews pointed at limitations of the model formulation, for instance, skews of l_1 and l_2 were pushing a(9,5) to negative values, and skew in l_6 pushed a(11,7) to be larger than one, which was unrealistic. Lastly, observed SOC contributed little information for C partitioning from leaves to surface metabolic litter (w_1) and C partitioning from soil microbial to passive pool if no sand or clay content (t_5).

After parameter calibration temperature sensitivity, Q_{10}, decreased from 2 to 1.84 (with 95% CI of 1.75–1.99); clay effects on partitioning coefficients were increased, whereas the effects of lignin and labile C fractions were decreased (Table 1). Less carbon reached slow pool from surface litter and soil litter (Figure 1), which, in combination with the decreased optimum slow pool's residence time, decreased the size of the slow pool from 361 Pg to 275 Pg (95% CI 205–459 Pg). Soil microbial and passive pools, on the contrary, increased. Soil microbial pool increased from 10.6 Pg to 11.8 Pg (95% CI 9.2–18.1 Pg) due to higher partitioning coefficient from soil litter and lower Q_{10}. Passive pool increased from 346 Pg to 865 Pg (95% CI 735–1047 Pg), and the change was due to increase in its residence time (Figure 1) and decrease in Q_{10}.

Calibrated parameters also showed that, compared to original parameters, a higher fraction of the fine root carbon was allocated to the structural litter, and a lower fraction was allocated to the metabolic litter (Figure 1). Increase in the above mentioned C allocation coefficient to soil structural litter together with lower Q_{10} led to an overall increase in soil litter pool due to longer C residence time in the soil structural than soil metabolic litter pool. In accordance with C cycle theory [*Luo and Zhou*, 2006], larger soil litter pool contributed more C to the soil pool, which in combination with lower C partitioning from surface litter to soil led to a shift in importance of C inputs from surface and belowground litter for SOC pool formation. For instance, the initial ratio of soil

Table 2. Correlations Between the Calibrated Parameters[a]

Parameter Correlations																														
c(11,11)	1.00																													
c(12,12)	−0.04	1.00																												
Q_{10}	0.10	0.21	1.00																											
l_1	0.05	−0.01	0.19	1.00																										
l_2	−0.03	−0.01	−0.09	0.07	1.00																									
l_3	0.07	0.14	0.25	−0.09	0.04	1.00																								
l_4	0.02	0.03	−0.20	0.04	−0.05	0.03	1.00																							
l_5	−0.07	−0.04	0.30	−0.01	0.07	−0.04	0.02	1.00																						
l_6	−0.02	0.08	−0.27	−0.06	−0.01	−0.01	−0.08	0.14	1.00																					
t_1	0.00	0.07	−0.15	−0.09	−0.02	−0.05	0.01	0.03	−0.10	1.00																				
t_2	−0.03	−0.23	−0.07	0.04	−0.01	0.02	−0.02	−0.03	−0.05	−0.12	1.00																			
t_3	0.01	−0.07	0.07	0.10	−0.05	0.01	0.02	−0.02	−0.06	−0.02	0.06	1.00																		
t_4	0.06	0.10	−0.22	−0.06	0.08	−0.14	0.02	−0.02	0.11	0.13	−0.01	0.13	1.00																	
t_5	0.00	−0.03	−0.06	0.00	0.03	−0.03	0.08	−0.03	−0.07	0.04	0.00	0.00	0.01	1.00																
t_6	0.13	0.30	−0.05	−0.08	0.05	−0.04	−0.01	0.11	0.07	−0.08	−0.15	−0.56	0.30	−0.04	1.00															
t_7	0.01	0.80	−0.01	−0.17	0.11	−0.01	0.02	0.01	0.09	0.01	−0.38	−0.14	0.37	−0.02	0.55	1.00														
t_8	0.00	0.32	−0.07	−0.03	0.03	0.03	0.01	−0.05	0.03	0.00	−0.05	−0.05	−0.05	0.00	−0.05	0.17	1.00													
t_9	0.07	−0.08	−0.26	−0.06	0.01	−0.15	−0.01	−0.05	0.06	0.00	0.05	−0.12	0.07	−0.04	−0.30	−0.26	−0.11	1.00												
w_1	0.08	0.05	0.29	−0.19	0.02	0.00	−0.09	0.01	−0.03	−0.07	−0.05	−0.08	0.05	−0.02	0.00	0.00	−0.03	−0.03	1.00											
w_2	−0.01	−0.11	0.15	−0.08	−0.07	0.02	−0.10	0.04	−0.06	0.02	0.03	0.01	−0.13	0.01	−0.04	−0.13	−0.07	0.00	0.09	1.00										
	c(11,11)	c(12,12)	Q_{10}	l_1	l_2	l_3	l_4	l_5	l_6	t_1	t_2	t_3	t_4	t_5	t_6	t_7	t_8	t_9	w_1	w_2										

[a]The darker the shade of the cell the stronger is the correlation between the parameters. The strongest positive correlations were between passive C pool turnover and clay effect on partitioning from slow pool and passive pool, and between sand effect on C partitioning from soil microbial C pool to passive pool and clay effect on partitioning from slow pool to passive pool. The strongest negative correlations were between sand effect on C partitioning from soil microbial C pool to passive pool and sand effect on C partitioning from soil microbial C pool to slow pool.

structural litter to surface structural litter inputs into soil slow pool was 0.66, and after parameter optimization the ratio became 6.69. Thus, soil litter contribution to slow soil C pool formation was more important than that modeled originally. The implication of more root inputs rather than shoot inputs into soil C pool is supported by long-term experimental [*Kätterer et al*., 2011] and meta-analysis [*Rasse et al*., 2005] studies.

3.3. Parameter Correlations

We used the posterior distributions to calculate correlations among the model parameters (Table 2). Out of 190 parameter pairs, three pairs had strong correlations. The strongest positive correlations were between passive C pool turnover, c(12,12), and clay effect on partitioning from slow to passive pool, t_7; and between sand effect on C partitioning from soil microbial to passive pool, t_6, and t_7. The strongest negative correlation was between t_6 and sand effect on C partitioning from soil microbial C pool to slow pool, t_3.

3.4. Improvement of Soil Carbon Estimation With Data Assimilation

After parameter calibration, the fitness between observed and modeled SOC improved substantially (Figures 3b and 3c): calibrated model explained 41% of the variability in the observed SOC whereas uncalibrated model explained 27%. The model with calibrated parameters also reduced the magnitude of the average underprediction to 2.1 kg/m^2 and decreased RMSE by 38%. Using posterior parameter distributions we generated the standard deviations of SOC for each grid cell to illustrate the uncertainty in the estimated SOC. The regions with the highest uncertainties were located in the northern latitudes and tropics (Figure 3d). Global SOC content in CLM-CASA' increased from 762 Pg to 1205 Pg (with 95% CI of 1150–1293 Pg) after data assimilation. The global SOC range was within the 95% CI of the observed HWSD SOC estimates presented by *Todd-Brown et al*. [2013], however, it was still lower than global observed soil C content in IGBP-DIS.

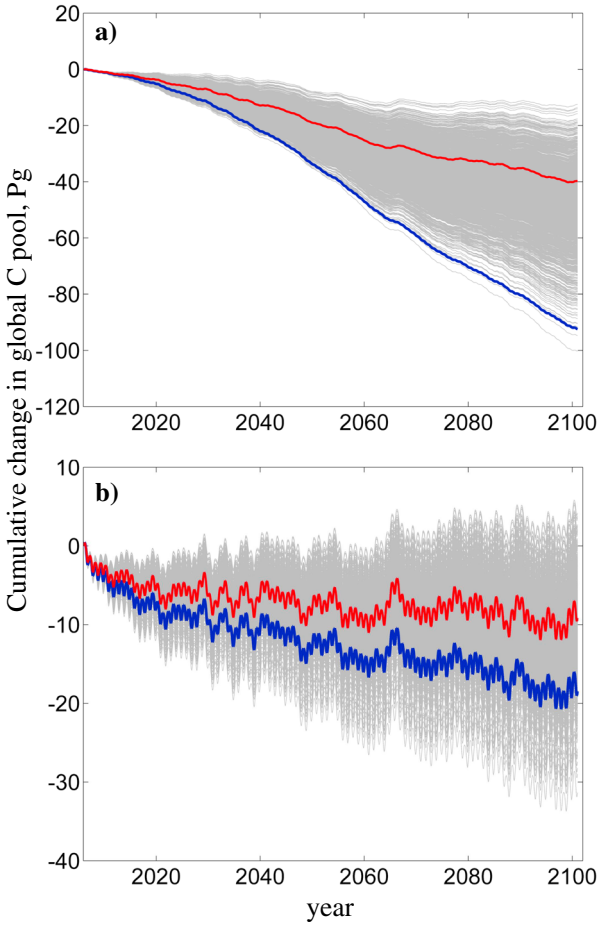

Figure 5. Change in CLM-CASA's (a) soil and (b) litter carbon under RCP 8.5 climate change scenario. Blue lines are projections of the model with original parameters, red lines, model with maximum likelihood parameters, and gray lines are projections of the models with parameter samples from the posterior distributions (sample size = 2000), representing the uncertainties of projections. Soils released 45 Pg C less in the model with calibrated parameters than the model with original parameters. Similarly, litter released 6.5 Pg C less in the calibrated model's projections than in the original model's projection. Despite the differences in models' projections, the original model's projections were within the uncertainty range.

3.5. Carbon Pool Responses to Environmental Change

To illustrate the impact of parameter calibration, we performed the forward runs using a climate change scenario (RCP8.5). Over 95 years, soils in the calibrated model released 48 Pg C less than soils in the original model (Figure 5a). Similarly, carbon loss from litter decreased by 6.5 Pg in the calibrated model, compared to the original model (Figure 5b). The decreases in the C loss rates in litter and soil C pools were caused by reduction in temperature sensitivity. The decreased soil C loss was also caused by the decrease in the calibrated passive pool's turnover rate. We also generated the uncertainties of changes in C pools from the posterior parameter distributions to gain perspective about the magnitude of the range for the cumulative C change after 95 years (gray lines in Figure 5). The uncertainty ranges were quite large: from 15 to 100 Pg for cumulative soil C loss, and from −30 to +5 Pg for cumulative litter C change. The magnitude of uncertainties was caused mostly by the uncertainties in maximum turnover rates and Q_{10}, as soil C dynamics was most sensitive to those parameters [*Post et al.*, 2008].

4. Discussion

4.1. Current Status of Soil Carbon Modeling

Currently, most carbon cycle models are similarly formulated: they partition the photosynthetically fixed C among the live and dead carbon pools, from which C is released via autotrophic or heterotrophic respiration [*Todd-Brown et al.*, 2012; *Weng and Luo*, 2011]. Despite the conceptual similarity of the models, their estimates of global soil C range from 514 to 3046 Pg with poor spatial correlation with the empirical estimates (up to $r^2 = 0.16$) [*Todd-Brown et al.*, 2012]. While the C influx is an important determinant of the C pool size, the capacity and sustainability of a C sink (e.g., soil C sink) under changing environmental conditions are strongly regulated by the C sink's residence time [*Luo et al.*, 2001, 2003], hence, it is important to calibrate the parameters regulating it.

Since the start of global soil C map production in 1982 [*Post et al.*, 1982], to our knowledge, only very few studies have made an attempt to use global soil C distributions to constrain global soil C residence times. For example, *Zhou et al.* [2009] and *Ise and Moorcroft* [2006] used the IGBP-DIS data set [*Group*, 2000] to constrain global soil C temperature sensitivities, and *Smith et al.* [2013] developed the C cycle model constrained with multiple data streams. This study showed that the poor model performance in simulating soil C could be substantially improved via parameter calibration against the observed soil C data. To model the C cycle as realistically as possible, we not only need to incorporate more processes into ESMs as the modeling community currently focuses on [*Koven et al.*, 2009; *Koven et al.*, 2011; *Lawrence et al.*, 2011; *Luo et al.*, 2009] but also need to develop our capacity to calibrate parameters effectively against the observed data.

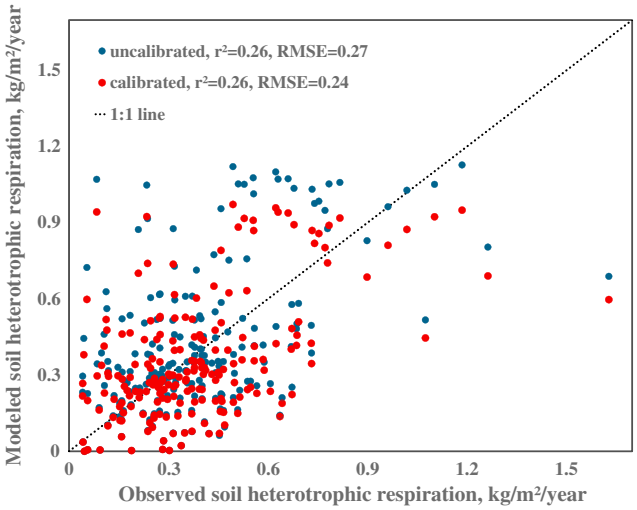

Figure 6. Point-by-point comparison of the modeled soil heterotrophic respiration to the observed data derived from *Bond-Lamberty and Thomson* [2012]. Parameter calibration did not change the explained variability in the observations; it reduced the RMSE by 10%.

4.2. Improvement of Soil Carbon Modeling

Our results showed that applying data assimilation could greatly reduce the mismatches between modeled and observed soil C. This error reduction was achieved largely due to increase in the soil C residence times. The implication that residence time in the original model was too low was in agreement with literature. For instance, *Rumpel and Kögel-Knabner* [2011] reported isotope-derived passive C pools' residence times for the top meter of different soil types ranging from 1026 years to 3030 years with samples from South America, Australia, Eurasia, and Africa. In comparison, the original model underestimated passive pool C residence time by 42–2046 years, whereas the calibrated model produced an estimate closer to the reported values (global average C residence time of passive pool was 2627 years with 95% CI 1583–3581 years).

To generate the estimates comparable to the ones in *Todd-Brown et al*. [2013], we calculated global weighted averages of soil residence time as the ratio of soil C pool to NPP. After parameter calibration, soil C residence time increased from 14 to 26 years (with 95% CI 25–28 years), which was within the range of observed soil C residence times reported in *Todd-Brown et al*. [2013]. We then calculated soil C residence time as the ratio of soil C pool to soil heterotrophic respiration and observed that global mean residence time increased from 32.3 years to 51 years (95% CI 45–61 years). The posterior estimates were too high compared to a global soil residence time of 32 years reported in *Raich and Schlesinger* [1992]. However, in the above mentioned study, soil residence time was obtained with the assumption that 30% of soil respiration originated from roots, which was lower than the average global estimate derived from *Bond-Lamberty and Thomson* [2010] (54%). We corrected the assumption in *Raich and Schlesinger* [1992] and SOC residence time became 48.6 years, which was within the 95% CI for our calibrated estimate. Combining more up-to-date range of estimates for SOC [*Todd-Brown et al*., 2013] and global soil respiration [*Bond-Lamberty and Thomson*, 2010], we obtained a range for global soil residence times of 16.5 to 41 years, which was outside of our posterior 95% CI. Such spread in the observed estimates highlights the need for data sets with better confidence.

We tested how new residence times affected C flux predictions by comparing the modeled soil heterotrophic respiration to the observed values from *Bond-Lamberty and Thomson* [2010, 2012]. The global observed range for soil heterotrophic respiration (calculated from soil respiration) was 41–54 Pg/year. Both model predictions were within the observed estimates: original model simulated soil heterotrophic respiration at 46 Pg/year and calibrated model predicted 40 Pg/year with 95% CI 36–52 Pg/year. The spatial predictions of the calibrated model were significantly different from the original model ($P < 0.05$), and although there was no improvement in the explained variability of the observed data after calibration, RMSE reduced by 10% (Figure 6). The decrease of soil respiration was a logical outcome of the decrease in Q_{10} and maximum turnover rate of soil passive pool although the latter is somewhat offset by the increase of maximum turnover rate in slow pool. The lack of large improvement in prediction of the observed soil heterotrophic respiration may be due to interannual variability of the observations, which was not accounted for as we assumed equilibrium conditions for the purpose of parameter calibration; differences in scale (model grid was around 2.8 by 2.8°, whereas the observation was a point on a grid); and limitations in model structure, which was also indicated by parameters approaching unrealistic values by skewing against their maxima or minima.

The large role of chemical stabilization in soil C pool formation illustrated by increase in clay effect on C partitioning to more recalcitrant pools has been supported by the observations and is described in the

literature [*Krull et al*., 2003; *Paul et al*., 2008; *Torn et al*., 1997]. Parameter calibration also revealed a larger regulation of soil C by soil litter inputs than surface litter inputs, which was also supported by experimental results [*Kätterer et al*., 2011; *Rasse et al*., 2005]. Hence, through model calibration we were able to not only improve the fitness between modeled and observed soil C but also gain insights into the C cycle processes.

4.3. Uncertainty in Future C Projections

With the prospect of global warming it is important to constrain the magnitude of SOC feedback (which depends on SOC residence time) as fast CO_2 release from soils may accelerate the increases in temperature. We discussed earlier that parameter calibration decreased both the maximum turnover rate and temperature sensitivity of SOC. Our maximum likelihood temperature sensitivity was within the range of the estimates constrained against the atmospheric CO_2 concentrations by *Jones and Cox* [2001] (2.1 ± 0.7 and 0.91 ± 0.4); higher than the average global Q_{10} reported in *Zhou et al*. [2009] (1.72); and higher than the estimate in *Ise and Moorcroft* [2006] (1.37). The Q_{10} from *I*se in Moorcroft [2006], however, was likely underestimated as authors used NPP rather than C influx from litter for SOC input. According to Figure S1, a higher input would decrease residence time for the same SOC under equilibrium conditions. The range in the posterior SOC residence times caused large uncertainties in the cumulative soil C change (a 15–100 Pg loss), which was within the range reported in *Smith et al*. [2013] (from a 138 Pg C loss to a 82 Pg C gain). The smaller uncertainty range in this study did not indicate better constraint, it was most likely due to the lower number of parameters: the uncertainties in *Smith et al*. [2013] resulted from parameters regulating soil C dynamics as well as parameters regulating plants' carbon fixation. The large uncertainty ranges clearly indicated the need for additional data sets to further constrain model parameters.

5. Conclusion

We calibrated a global land model against the global observed soil C data set using Bayesian MCMC approach. By adjusting parameters that influenced residence times of C pools, we were able to substantially improve the fitness between observed and modeled soil C. After parameter calibration we discovered that the regions with the highest uncertainty in soil C were located in the northern latitudes and tropics, indicating that we need to put more efforts in model soil C dynamics in those regions. When propagated over time under RCP8.5 scenario posterior parameter uncertainties resulted in 15–100 Pg C loss from soils over 95 years; however, the maximum likelihood C loss (40 Pg) was 53% lower than SOC loss predicted with original parameters. Similarly, maximum likelihood litter loss decreased 53% from the original predictions, but the range of change was from a 30 Pg C loss to a 5 Pg C gain.

As we show in this study, data assimilation is a useful tool for gaining insights into carbon cycle modeling, identifying regions that need additional data collection and more research to improve representation of ecosystem carbon processes, as well as for uncertainty analysis of the model projections. More global level C cycle data (e.g., litter pools, litter residence times, soil C residence times, live C pools, and their residence times) along with their uncertainties are needed to constrain the processes in carbon cycle. Assimilating the data into the model at global level will constrain C cycle feedback and provide more confidence in the future carbon budget, which will facilitate more effective management of the natural resources.

Acknowledgments

This study was financially supported by U.S. Department of Energy, Terrestrial Ecosystem Sciences grant DE SC0008270 and U.S. National Science Foundation (NSF) grants DBI 0850290, EPS 0919466, DEB 0743778, DEB 0840964, and EF 1137293. Part of the model runs were performed at the Supercomputing Center for Education & Research (OSCER), University of Oklahoma. We acknowledge the World Climate Research Programme's Working Group on Coupled Modelling, which is responsible for CMIP, and we thank the climate modeling groups Community Earth System Model Contributors for producing and making available their model output. For CMIP the U.S. Department of Energy's Program for Climate Model Diagnosis and Intercomparison provides coordinating support and led development of software infrastructure in partnership with the Global Organization for Earth System Science Portals. We also thank three anonymous reviewers for helping us improve the manuscript.

References

Batjes, N. (1995), A homogenized soil data file for global environmental research: A subset of FAO, ISRIC and NCRS profiles.

Bond-Lamberty, B., and A. Thomson (2010), A global database of soil respiration data, *Biogeosciences*, *7*(6), 1915–1926, doi:10.5194/bg-7-1915-2010.

Bond-Lamberty, B., and A. Thomson (2012), A Global Database of Soil Respiration Data, Version 2.0, Data set. [Available at http://daac.ornl.gov] from Oak Ridge National Laboratory Distributed Active Archive Center, Oak Ridge, Tennessee, U.S.A., doi:10.3334/ORNLDAAC/1070.

Delire, C., J. A. Foley, and S. Thompson (2003), Evaluating the carbon cycle of a coupled atmosphere-biosphere model, *Global Biogeochem. Cycles*, *17*(1), 1012, doi:10.1029/2002GB001870.

FAO (1995), Digital soil map of the world and derived soil properties (version 3.5).

Freibauer, A., M. D. A. Rounsevell, P. Smith, and J. Verhagen (2004), Carbon sequestration in the agricultural soils of Europe, *Geoderma*, *122*(1), 1–23, doi:10.1016/j.geoderma.2004.01.021.

Friedlingstein, P., et al. (2006), Climate-carbon cycle feedback analysis: Results from the C4MIP model intercomparison, *J. Clim.*, *19*(14), 3337–3353, doi:10.1175/jcli3800.1.

Gelman, A., and D. B. Rubin (1992), Inference from iterative simulation using multiple sequences, *Stat. Sci.*, *7*, 457–511, doi:10.1214/ss/1177011136.

Gelman, A., G. Roberts, and W. Gilks (1996), Efficient metropolis jumping hules, *Bayesian Stat.*, *5*, 599–608.

Group, G. S. D. T. (2000), Global gridded surfaces of selected soil characteristics (IGBP-DIS), [Global Gridded Surfaces of Selected Soil Characteristics (International Geosphere-Biosphere Programme - Data and Information System)], Data set., Oak Ridge National Laboratory Distributed Active Archive Center, Oak Ridge, TN, U.S.A., doi:10.3334/ORNLDAAC/569.

Haario, H., E. Saksman, and J. Tamminen (2001), An adaptive Metropolis algorithm, *Bernoulli*, *7*, 223–242.

Harmon, R., and P. Challenor (1997), A Markov chain Monte Carlo method for estimation and assimilation into models, *Ecol. Modell.*, *101*(1), 41–59, doi:10.1016/S0304-3800(97)01947-9.

Houghton, J. T., Y. Ding, D. J. Griggs, M. Noguer, P. J. van der Linden, X. Dai, K. Maskell, and C. Johnson (2001), *Climate Change 2001: The Scientific Basis*, Cambridge Univ. Press, Cambridge, doi:10.1002/qj.200212858119.

House, J. I., I. Colin Prentice, and C. Le Quéré (2002), Maximum impacts of future reforestation or deforestation on atmospheric CO2, *Global Change Biol.*, *8*(11), 1047–1052, doi:10.1046/j.1365-2486.2002.00536.x.

Ise, T., and P. R. Moorcroft (2006), The global-scale temperature and moisture dependencies of soil organic carbon decomposition: An analysis using a mechanistic decomposition model, *Biogeochemistry*, *80*(3), 217–231, doi:10.1007/s10533-006-9019-5.

Jones, C. D., and P. M. Cox (2001), Constraints on the temperature sensitivity of global soil respiration from the observed interannual variability in atmospheric CO_2, *Atmos. Sci. Lett.*, *2*(1–4), 166–172, doi:10.1006/asle.2001.0044.

Kätterer, T., M. A. Bolinder, O. Andrén, H. Kirchmann, and L. Menichetti (2011), Roots contribute more to refractory soil organic matter than above-ground crop residues, as revealed by a long-term field experiment, *Agric. Ecosyst. Environ.*, *141*(1–2), 184–192, doi:10.1016/j.agee.2011.02.029.

Keenan, T. F., E. Davidson, A. M. Moffat, W. Munger, and A. D. Richardson (2012), Using model-data fusion to interpret past trends, and quantify uncertainties in future projections, of terrestrial ecosystem carbon cycling, *Global Change Biol.*, *18*(8), 2555–2569, doi:10.1111/j.1365-2486.2012.02684.x.

Keppel-Aleks, G., et al. (2013), Atmospheric carbon dioxide variability in the Community Earth System Model: Evaluation and transient dynamics during the twentieth and twenty-first centuries, *J. Clim.*, *26*(13), 4447–4475, doi:10.1175/JCLI-D-12-00589.1.

Kirschbaum, M. U. F. (1995), The temperature dependence of soil organic matter decomposition, and the effect of global warming on soil organic C storage, *Soil Biol. Biochem.*, *27*(6), 753–760, doi:10.1016/0038-0717(94)00242-S.

Koven, C., P. Friedlingstein, P. Ciais, D. Khvorostyanov, G. Krinner, and C. Tarnocai (2009), On the formation of high-latitude soil carbon stocks: Effects of cryoturbation and insulation by organic matter in a land surface model, *Geophys. Res. Lett.*, *36*, L21501, doi:10.1029/2009GL040150.

Koven, C. D., B. Ringeval, P. Friedlingstein, P. Ciais, P. Cadule, D. Khvorostyanov, G. Krinner, and C. Tarnocai (2011), Permafrost carbon-climate feedbacks accelerate global warming, *Proc. Natl. Acad. Sci. U.S.A.*, *108*(36), 14,769–14,774, doi:10.1073/pnas.1103910108.

Krull, E. S., J. A. Baldock, and J. O. Skjemstad (2003), Importance of mechanisms and processes of the stabilisation of soil organic matter for modelling carbon turnover, *Funct. Plant Biol.*, *30*(2), 207–222, doi:10.1071/FP02085.

Kucharik, C. J., J. A. Foley, C. Delire, V. A. Fisher, M. T. Coe, J. D. Lenters, C. Young-Molling, N. Ramankutty, J. M. Norman, and S. T. Gower (2000), Testing the performance of a dynamic global ecosystem model: Water balance, carbon balance, and vegetation structure, *Global Biogeochem. Cycles*, *14*(3), 795–825, doi:10.1029/1999GB001138.

Kuppel, S., P. Peylin, F. Chevallier, C. Bacour, F. Maignan, and A. D. Richardson (2012), Constraining a global ecosystem model with multi-site eddy-covariance data, *Biogeosciences*, *9*(10), 3757–3776, doi:10.5194/bg-9-3757-2012.

Lawrence, D., et al. (2011), Parameterization improvements and functional and structural advances in version 4 of the Community Land Model, *J. Adv. Model. Earth Syst.*, *3*, M03001, doi:10.1029/2011MS000045.

Lawrence, P. J., and T. N. Chase (2007), Representing a new MODIS consistent land surface in the Community Land Model (CLM 3.0), *J. Geophys. Res.*, *112*, G01023, doi:10.1029/2006JG000168.

Liski, J., T. Palosuo, M. Peltoniemi, and R. Sievänen (2005), Carbon and decomposition model Yasso for forest soils, *Ecol. Modell.*, *189*(1–2), 168–182, doi:10.1016/j.ecolmodel.2005.03.005.

Luo, Y. (2007), Terrestrial carbon-cycle feedback to climate warming, in *Annual Review of Ecology Evolution and Systematics*, pp. 683–712, Annual Reviews, Palo Alto, doi:10.1146/annurev.ecolsys.38.091206.095808.

Luo, Y., and E. Weng (2011), Dynamic disequilibrium of the terrestrial carbon cycle under global change, *Trends Ecol. Evol.*, *26*(2), 96–104, doi:10.1016/j.tree.2010.11.003.

Luo, Y., and X. Zhou (2006), *Soil Respiration and the Environment*, 1 ed., 328 pp., Academic Press, New York.

Luo, Y., L. Wu, J. A. Andrews, L. White, R. Matamala, K. V. R. Schäfer, and W. H. Schlesinger (2001), Elevated CO_2 differentiates ecosystem carbon processes: Deconvolution analysis of Duke Forest FACE data, *Ecol. Monogr.*, *71*(3), 357–376, doi:10.1890/0012-9615(2001)071[0357:ecdecp]2.0.co;2.

Luo, Y., L. W. White, J. G. Canadell, E. H. DeLucia, D. S. Ellsworth, A. Finzi, J. Lichter, and W. H. Schlesinger (2003), Sustainability of terrestrial carbon sequestration: A case study in Duke Forest with inversion approach, *Global Biogeochem. Cycles*, *17*(1), 1021, doi:10.1029/2002GB001923.

Luo, Y., E. Weng, X. Wu, C. Gao, X. Zhou, and L. Zhang (2009), Parameter identifiability, constraint, and equifinality in data assimilation with ecosystem models, *Ecol. Appl.*, *19*(3), 571–574, doi:10.1890/08-0561.1.

Marshall, L., D. Nott, and A. Sharma (2004), A comparative study of Markov chain Monte Carlo methods for conceptual rainfall-runoff modeling, *Water Resour. Res.*, *40*, W02501, doi:10.1029/2003WR002378.

Melillo, J. M., P. A. Steudler, J. D. Aber, K. Newkirk, H. Lux, F. P. Bowles, C. Catricala, A. Magill, T. Ahrens, and S. Morrisseau (2002), Soil warming and carbon-cycle feedbacks to the climate system, *Science*, *298*(5601), 2173–2176, doi:10.1126/science.1074153.

Mosegaard, K., and M. Sambridge (2002), Monte Carlo analysis of inverse problems, *Inverse Probl.*, *18*(3), R29–R54.

Oechel, W. C., G. L. Vourlitis, S. J. Hastings, R. C. Zulueta, L. Hinzman, and D. Kane (2000), Acclimation of ecosystem CO_2 exchange in the Alaskan Arctic in response to decadal climate warming, *Nature*, *406*(6799), 978–981, doi:10.1038/35023137.

Oleson, K. W., Y. Dai, G. Bonan, M. Bosilovich, R. Dickinson, P. Dirmeyer, F. Hoffman, P. Houser, S. Levis, and G.-Y. Niu (2004), Technical description of the community land model (CLM), *NCAR Tech. Note NCAR/TN-461+ STR*, 173.

Oleson, K. W., G. Niu, Z. Yang, D. Lawrence, P. Thornton, P. Lawrence, R. Stockli, R. Dickinson, G. Bonan, and S. Levis (2008), Improvements to the Community Land Model and their impact on the hydrological cycle, *J. Geophys. Res.*, *113*, G01021, doi:10.1029/2007JG000563.

Oleson, K. W., G. Niu, Z. Yang, D. Lawrence, P. Thornton, P. Lawrence, R. Stockli, R. Dickinson, G. Bonan, and S. Levis (2007), *CLM3. 5 Documentation*, 34 pp., National Center for Atmospheric Research, Boulder.

Olson, R., J. Scurlock, S. Prince, D. Zheng, and K. Johnson (2001), NPP multi-biome: NPP and driver data for ecosystem model-data intercomparison, Data set. [Available at http://www.daac.ornl.gov] from the Oak Ridge National Laboratory Distributed Active Archive Center, Oak Ridge, Tennessee, U.S.A.

Parton, W. J., et al. (1993), Observations and modeling of biomass and soil organic matter dynamics for the grassland biome worldwide, *Global Biogeochem. Cycles*, *7*(4), 785–809, doi:10.1029/93GB02042.

Parton, W. J., P. J. Hanson, C. Swanston, M. Torn, S. E. Trumbore, W. Riley, and R. Kelly (2010), ForCent model development and testing using the Enriched Background Isotope Study experiment, *J. Geophys. Res.*, *115*, G04001, doi:10.1029/2009JG001193.

Paul, S., H. Flessa, E. Veldkamp, and M. López-Ulloa (2008), Stabilization of recent soil carbon in the humid tropics following land use changes: Evidence from aggregate fractionation and stable isotope analyses, *Biogeochemistry*, *87*(3), 247–263, doi:10.1007/s10533-008-9182-y.

Post, J., F. F. Hattermann, V. Krysanova, and F. Suckow (2008), Parameter and input data uncertainty estimation for the assessment of long-term soil organic carbon dynamics, *Environ. Modell. Software*, *23*(2), 125–138, doi:10.1016/j.envsoft.2007.05.010.

Post, W. M., W. R. Emanuel, P. J. Zinke, and A. G. Stangenberger (1982), Soil carbon pools and world life zones, *Nature*, *298*(5870), 156–159, doi:10.1038/298156a0.

Raddatz, T. J., C. H. Reick, W. Knorr, J. Kattge, E. Roeckner, R. Schnur, K. G. Schnitzler, P. Wetzel, and J. Jungclaus (2007), Will the tropical land biosphere dominate the climate–carbon cycle feedback during the twenty-first century?, *Clim. Dyn.*, *29*(6), 565–574, doi:10.1007/s00382-007-0247-8.

Raich, J. W., and W. H. Schlesinger (1992), The global carbon dioxide flux in soil respiration and its relationship to vegetation and climate, *Tellus, Ser. B*, *44*(2), 81–99, doi:10.1034/j.1600-0889.1992.t01-1-00001.x.

Randerson, J. T., et al. (2009), Systematic assessment of terrestrial biogeochemistry in coupled climate–carbon models, *Global Change Biol.*, *15*(10), 2462–2484, doi:10.1111/j.1365-2486.2009.01912.x.

Rasse, D., C. Rumpel, and M.-F. Dignac (2005), Is soil carbon mostly root carbon? Mechanisms for a specific stabilisation, *Plant Soil*, *269*(1–2), 341–356, doi:10.1007/s11104-004-0907-y.

Rayner, P. J., M. Scholze, W. Knorr, T. Kaminski, R. Giering, and H. Widmann (2005), Two decades of terrestrial carbon fluxes from a carbon cycle data assimilation system (CCDAS), *Global Biogeochem. Cycles*, *19*, GB2026, doi:10.1029/2004GB002254.

Roeckner, E., G. Bäuml, L. Bonventura, R. Brokopf, M. Esch, M. Giorgetta, S. Hagemann, I. Kirchner, L. Kornblueh, and E. Manzini (2003), The atmospheric general circulation model ECHAM5. PART I: Model description, *Report 349*, Max Planck Institute for Meteorology, Hamburg, Germany.

Rumpel, C., and I. Kögel-Knabner (2011), Deep soil organic matter—A key but poorly understood component of terrestrial C cycle, *Plant Soil*, *338*(1–2), 143–158, doi:10.1007/s11104-010-0391-5.

Rustad, L. R., J. Campbell, G. Marion, R. Norby, M. Mitchell, A. Hartley, J. Cornelissen, J. Gurevitch, and Gcte-News (2001), A meta-analysis of the response of soil respiration, net nitrogen mineralization, and aboveground plant growth to experimental ecosystem warming, *Oecologia*, *126*(4), 543–562, doi:10.1007/s004420000544.

Smith, M. J., D. W. Purves, M. C. Vanderwel, V. Lyutsarev, and S. Emmott (2013), The climate dependence of the terrestrial carbon cycle, including parameter and structural uncertainties, *Biogeosciences*, *10*(1), 583–606, doi:10.5194/bg-10-583-2013.

Taylor, K. E., R. J. Stouffer, and G. A. Meehl (2011), An overview of CMIP5 and the experiment design, *Bull. Am. Meteorol. Soc.*, *93*(4), 485–498, doi:10.1175/BAMS-D-11-00094.1.

Thum, T., et al. (2011), Soil carbon model alternatives for ECHAM5/JSBACH climate model: Evaluation and impacts on global carbon cycle estimates, *J. Geophys. Res.*, *116*, G02028, doi:10.1029/2010JG001612.

Todd-Brown, K. E. O., J. T. Randerson, W. M. Post, F. M. Hoffman, C. Tarnocai, E. A. G. Schuur, and S. D. Allison (2012), Causes of variation in soil carbon predictions from CMIP5 Earth system models and comparison with observations, *Biogeosci. Discuss.*, *9*(10), 14,437–14,473, doi:10.5194/bgd-9-14437-2012.

Todd-Brown, K. E. O., J. T. Randerson, W. M. Post, F. M. Hoffman, C. Tarnocai, E. A. G. Schuur, and S. D. Allison (2013), Causes of variation in soil carbon simulations from CMIP5 Earth system models and comparison with observations, *Biogeosciences*, *10*(3), 1717–1736, doi:10.5194/bg-10-1717-2013.

Torn, M. S., S. E. Trumbore, O. A. Chadwick, P. M. Vitousek, and D. M. Hendricks (1997), Mineral control of soil organic carbon storage and turnover, *Nature*, *389*(6647), 170–173, doi:10.1038/38260.

Wang, Y. P., D. Baldocchi, R. A. Y. Leuning, E. V. A. Falge, and T. Vesala (2007), Estimating parameters in a land-surface model by applying nonlinear inversion to eddy covariance flux measurements from eight FLUXNET sites, *Global Change Biol.*, *13*(3), 652–670, doi:10.1111/j.1365-2486.2006.01225.x.

Weng, E., and Y. Luo (2011), Relative information contributions of model vs. data to short- and long-term forecasts of forest carbon dynamics, *Ecol. Appl.*, *21*(5), 1490–1505, doi:10.1890/09-1394.1.

Wu, X., Y. Luo, E. Weng, L. White, Y. Ma, and X. Zhou (2009), Conditional inversion to estimate parameters from eddy-flux observations, *J. Plant Ecol.*, *2*(2), 55–68, doi:10.1093/jpe/rtp005.

Xia, J., Y. Luo, Y. Wang, E. Weng, and O. Hararuk (2012), A semi-analytical solution to accelerate spin-up of a coupled carbon and nitrogen land model to steady state, *Geosci. Model Dev.*, *5*(5), 1259–1271, doi:10.5194/gmd-5-1259-2012.

Xia, J., Y. Luo, Y. P. Wang, and O. Hararuk (2013), Traceable components of terrestrial carbon storage capacity in biogeochemical models, *Global Change Biol.*, *19*, 2104–2116, doi:10.1111/gcb.12172.

Xu, T., L. White, D. Hui, and Y. Luo (2006), Probabilistic inversion of a terrestrial ecosystem model: Analysis of uncertainty in parameter estimation and model prediction, *Global Biogeochem. Cycles*, *20*, GB2007, doi:10.1029/2005GB002468.

Zhou, T., and Y. Luo (2008), Spatial patterns of ecosystem carbon residence time and NPP-driven carbon uptake in the conterminous United States, *Global Biogeochem. Cycles*, *22*, GB3032, doi:10.1029/2007GB002939.

Zhou, T., P. Shi, D. Hui, and Y. Luo (2009), Global pattern of temperature sensitivity of soil heterotrophic respiration (*Q*10) and its implications for carbon-climate feedback, *J. Geophys. Res.*, *114*, G02016, doi:10.1029/2008JG000850.